Hindawi Publishing Corporation
Journal of Nanomaterials
Volume 2013, Article ID 679638, 6 pages
http://dx.doi.org/10.1155/2013/679638

Research Article

Z-Contrast STEM Imaging of Long-Range Ordered Structures in Epitaxially Grown CoPt Nanoparticles

Kazuhisa Sato,[1] Keigo Yanajima,[2] and Toyohiko J. Konno[1]

[1] *Institute for Materials Research, Tohoku University, 2-1-1 Katahira, Aoba-ku, Sendai 980-8577, Japan*
[2] *Department of Materials Science, Tohoku University, 6-6 Aramaki, Aoba-ku, Sendai 980-8579, Japan*

Correspondence should be addressed to Kazuhisa Sato; ksato@imr.tohoku.ac.jp

Received 15 March 2013; Accepted 17 May 2013

Academic Editor: Takeshi Seki

We report on atomic structure imaging of epitaxial $L1_0$ CoPt nanoparticles using chemically sensitive high-angle annular dark-field scanning transmission electron microscopy (HAADF-STEM). Highly ordered nanoparticles formed by annealing at 973 K show single-variant structure with perpendicular *c*-axis orientation, while multivariant ordered domains are frequently observed for specimens annealed at 873 K. It was found that the (001) facets of the multivariant particles are terminated by Co atoms rather than by Pt, presumably due to the intermediate stage of atomic ordering. Coexistence of single-variant particles and multivariant particles in the same specimen film suggests that the interfacial energy between variant domains be small enough to form such structural domains in a nanoparticle as small as 4 nm in diameter.

1. Introduction

Recent developments in ultrahigh-density magnetic storage technology rely on novel recording media with high magnetocrystalline anisotropy energy (MAE) together with high-performance giant magnetoresistive (GMR) heads [1–4]. For such a purpose, CoPt alloy nanoparticles with the $L1_0$-type ordered structure are one of the candidate materials [5, 6]. The hard magnetic property of this alloy is attributed to the tetragonal $L1_0$-type ordered structure with a high MAE [7]: the reported value is as high as 4.1×10^6 J/m^3 for a single-crystal bulk $L1_0$-$Co_{50}Pt_{50}$ alloy [8]. The $L1_0$-type ordered structure is composed of alternate stacking of Co(001) and Pt(001) atomic planes in the [001] direction (*c*-axis). Since MAE is dependent on the long-range order (LRO) parameter [9, 10], atomic ordering and the stability of the ordered phase are key issues for hard magnetic properties of the $L1_0$-type magnetic alloy nanoparticles [11]. To extract chemical information directly related to the LRO in the atomic scale resolution, atomic number (Z) contrast imaging by high-angle annular dark-field scanning transmission electron microscopy (HAADF-STEM) is quite useful. One of the authors demonstrated the detection of nanometer-sized local atomic order in FePd nanoparticles by Z-contrast at an intermediate stage of the ordering process [12]. To date, detection of atomic ordering has been reported for several ordered alloy nanoparticles produced by different fabrication methods [13–16]. However, there is no report on the Z-contrast imaging of highly ordered epitaxial $L1_0$ CoPt nanoparticles so far.

In this study, we hence intend to characterize the atomic structure of highly ordered $L1_0$ CoPt nanoparticles using chemically sensitive atomic resolution HAADF-STEM. Large atomic number difference between Co ($Z = 27$) and Pt ($Z = 78$) enables clear visualization of atomic ordering in bimetallic CoPt nanoparticles; that is, Z-contrast makes the direct interpretation of image contrasts possible due to incoherent imaging nature [17].

2. Experimental

CoPt nanoparticles were fabricated by sequential electron-beam deposition of Pt and Co onto NaCl(001) substrates with a base pressure of 9×10^{-7} Pa [18]. The substrate temperature was kept at 653 K during the deposition. A quartz thickness monitor located near the substrate stage in the vacuum chamber was used to estimate and control the nominal

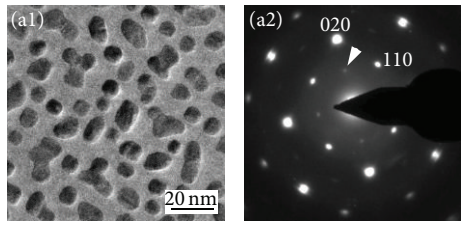

(a)

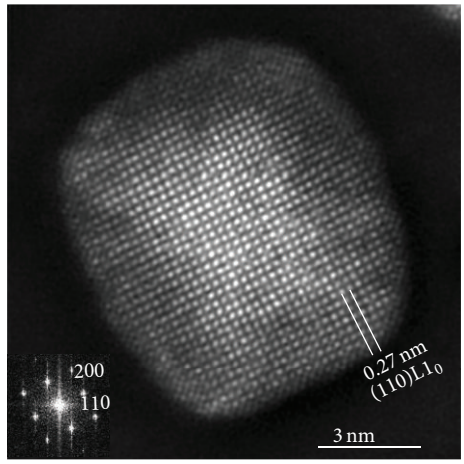

(b)

Figure 1: (a) BF-TEM image and corresponding SAED pattern of CoPt nanoparticles after annealing at 973 K for 100 min (sample no. 1). (b) HAADF-STEM image of a CoPt nanoparticle with the $L1_0$-type ordered structure. FFT pattern is shown in the inset.

thickness of deposited layers. We first deposited Pt to partially cover the substrate, which resulted in the formation of ⟨100⟩ oriented Pt islands. Next, Co was deposited onto the substrate with Pt followed by the deposition of an amorphous (a-) Al_2O_3 protective layer. In this sequential deposition process, Pt nanoparticles act as nucleation sites for Co nanoparticles [18, 19]. The deposition rates of Pt, Co, and Al_2O_3 were, respectively, 0.04, 0.2, and 0.3 nm/min. Nominal thickness and other detailed conditions for the sample preparation are listed in Table 1. After the deposition of Al_2O_3, the specimen films were then heated inside the vacuum chamber at 823 K for 3 h to promote island growth of nanoparticles. A part of the specimen film was then removed from the NaCl substrate by the immersion into distilled water, and floating film was mounted onto a Mo grid with a holey carbon film for TEM observation. To obtain highly ordered nanoparticles, we carried out high-temperature postdeposition annealing of the as-deposited film on a Mo grid at 873 or 973 K in a high-vacuum furnace ($<2 \times 10^{-5}$ Pa). Cooling rate after the heat treatment was set to be less than 3 K/min in order to ensure atomic ordering in small nanoparticles [18, 20]. STEM images were obtained using an FEI TITAN80-300 (STEM) operating at 300 kV with a field emission gun. We set beam convergence to be 10 mrad in half angle, taking into account the spherical aberration coefficient (1.2 mm) of the prefield of objective lens. *Z*-contrast images were acquired by using a HAADF-detector (Fischione model 3000) with detector half angles between 60 and 210 mrad. STEM images were simulated using QSTEM software [21]. Alloy compositions were analyzed by energy dispersive X-ray spectrometer (EDS) attached to the TEM.

3. Results and Discussion

Figure 1(a) shows a bright-field (BF) TEM image and a corresponding selected area electron diffraction (SAED) pattern of the Co-55 at %Pt nanoparticles after annealing at 973 K for 100 min (sample no. 1). Note that the annealing temperature of 973 K is 100 K lower than the order-disorder transformation temperature for the corresponding bulk alloy (Co-55 at %Pt) [22]. CoPt nanoparticles with the $L1_0$-type ordered structure were formed as epitaxial islands on the NaCl(001) substrate. The orientation relationships between CoPt and NaCl(001) is $\langle 100\rangle_{CoPt} \parallel \langle 100\rangle_{NaCl}, \{001\}_{CoPt} \parallel \{001\}_{NaCl}$ [18]. Strong 110 superlattice reflections of the $L1_0$ ordered structure indicates preferential growth of nanoparticles with the crystallographic *c*-axis oriented normal to the substrate surface (c-domain) with a high degree of order. In addition, the arrowhead indicates 001 superlattice reflection from nanoparticles with the *c*-axis oriented parallel to the substrate surface (a or b domain), while its intensity is quite weak compared to that of the 110 reflection.

Figure 1(b) shows a high-resolution HAADF-STEM image of a 10 nm sized $L1_0$ CoPt nanoparticle with the *c*-axis oriented normal to the film plane. Fast Fourier transform (FFT) pattern is also shown in the inset. Periodic arrangement of atoms by atomic order can be seen clearly as bright contrasts. It is obvious that the particle is single crystal as indicated by clear-cut (110) superlattice atomic planes which spread over the particle. In this specimen film, most of the particles observed were single crystal. Image contrasts of the (110) superlattice fringes are lower in the peripheral regions than those in the central part of the nanoparticle. To clarify the origin of such contrast variation, we performed image simulation using a model cluster.

Figure 2(a) shows a structure model and a simulated HAADF-STEM image of a fully ordered CoPt nanoparticle. The model is a truncated octahedron (TO) composed of 8000 atoms, 5.7 nm in width and 5.5 nm in height. As seen, contrast variation from the particle center to the {111} or {100} facets is reproduced in the simulated image of the fully ordered CoPt nanoparticle. Figure 2(b) shows intensity profiles of the simulated images measured in the [100] direction (b1) and $[1\bar{1}0]$ direction (b2). Intensity degradation towards {111} facet (B-B′) is prominent compared to that of {100} (A-A′) due to the thickness reduction. Thus, image simulation revealed that experimentally observed degradation of image contrast can be attributed to the thickness reduction in the peripheral region due to particle shape. This result indicates that HAADF-STEM image intensity is also sensitive to thickness variation in addition to atomic number. Similar degradation of image contrast has been observed in high-resolution TEM (HRTEM) images to a lesser degree compared to *Z*-contrast [18].

Figure 3(a) shows another example of HAADF-STEM image of a highly ordered CoPt nanoparticle after annealing

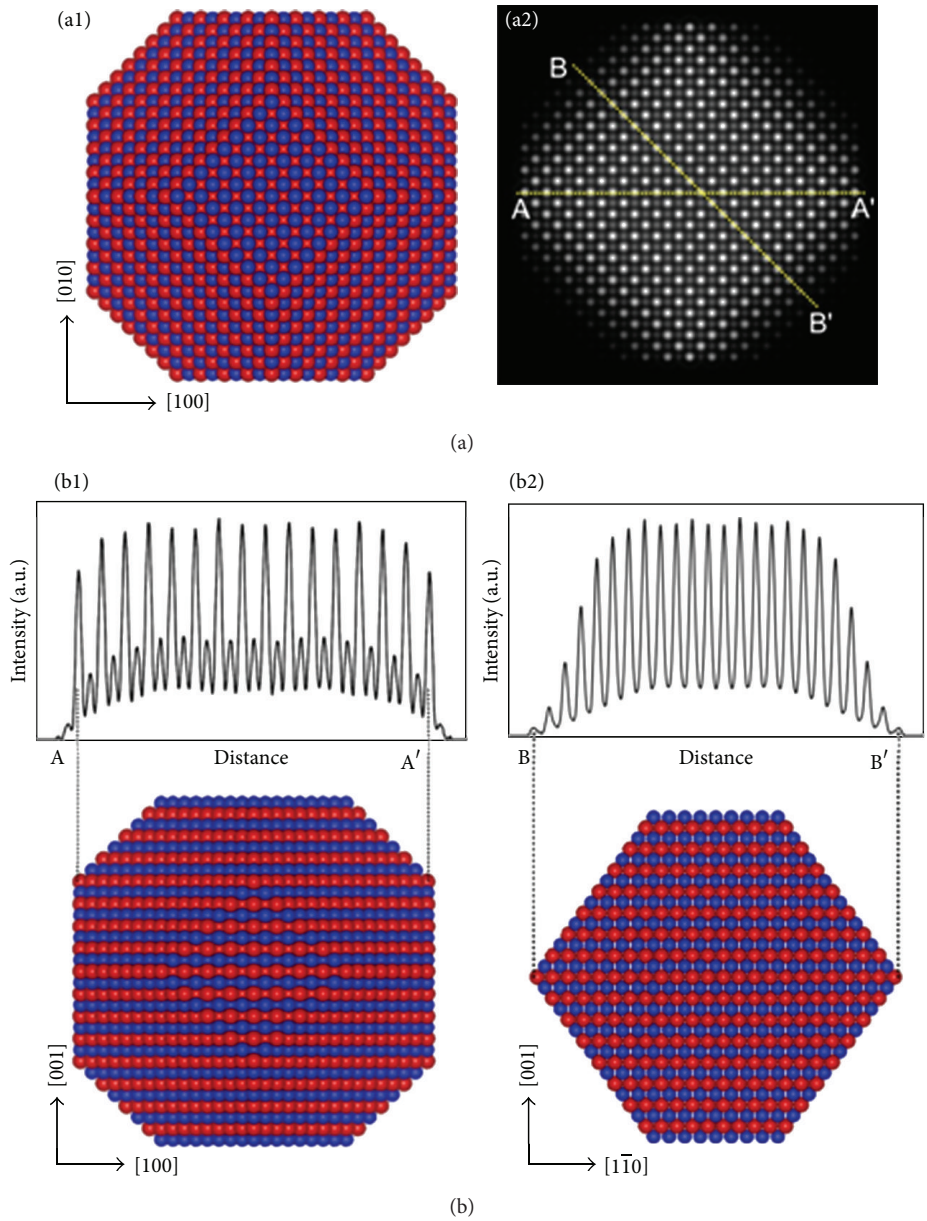

Figure 2: (a) A structure model (truncated octahedron) and a simulated HAADF-STEM image. The beam incidence is [001]. (b) Intensity profiles of simulated images measured in the [100] (b1) and [1$\bar{1}$0] directions (b2).

Table 1: Nominal thickness, alloy composition, annealing condition, and particle size for CoPt nanoparticles grown on NaCl(001) single-crystal substrates.

Sample no.	Nominal thickness	Composition	Annealing (cooling rate)	Particle size ($\ln \sigma$)
No. 1	Al_2O_3 (6.0 nm)/Co (0.7 nm)/Pt (1.0 nm)	55 at % Pt	973 K-100 min (2.8 K/min)	8.4 nm (0.15)
No. 2	Al_2O_3 (6.0 nm)/Co (0.7 nm)/Pt (1.0 nm)	55 at % Pt	873 K-10 h (2.4 K/min)	8.3 nm (0.20)
No. 3	Al_2O_3 (6.0 nm)/Co (0.15 nm)/Pt (0.20 nm)	61 at % Pt	873 K-1 h (1.5 K/min)	4.0 nm (0.13)

at 973 K for 100 min (sample no. 1). Particle size is 8 nm in diameter. The particle is single crystalline, and clear (110) superlattice atomic planes of the $L1_0$ ordered structure can be seen as bright contrasts. The (220) atomic planes are also resolved as shown in the upper inset. Two types of bright dots, strong and weak, correspond to Pt and Co atomic columns, respectively. Due to the alternate stacking of Co and Pt in the [001] direction of the $L1_0$ structure, the (220) atomic planes also possess an alternate stacking sequence of Co and Pt in the [110] direction. Thus, chemical sensitivity

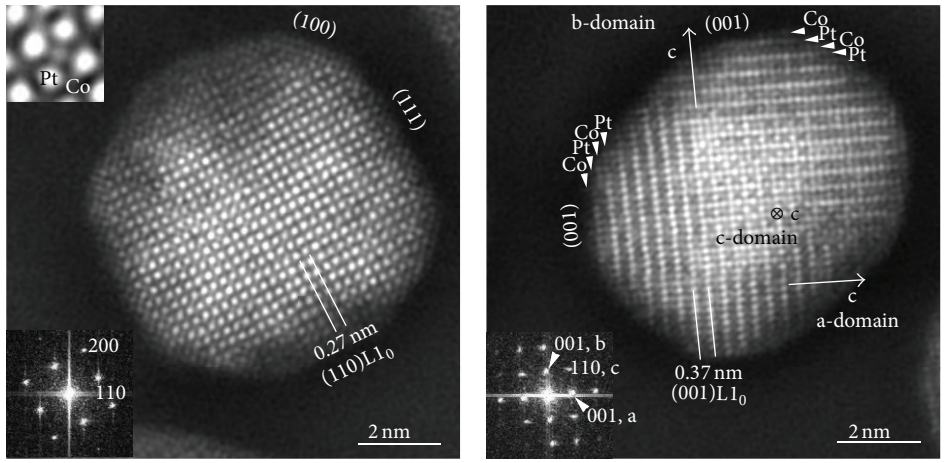

(a) (b)

Figure 3: HAADF-STEM images and corresponding FFT patterns of $L1_0$-CoPt nanoparticles: (a) single-crystal nanoparticle formed after annealing at 973 K for 100 min (sample no. 1). Magnified image is shown in the upper inset. (b) Nanoparticle composed of three-variant domains formed after annealing at 873 K for 10 h (sample no. 2).

of HAADF-STEM is quite useful to detect atomic ordering, while quantitative interpretation such as order parameter analysis is not straightforward. For this purpose, nanobeam electron diffraction can be employed under several prerequisite conditions [23].

On the other hand, for a specimen after annealing at 873 K for 10 h (sample no. 2), multivariant ordered domains were observed as well as single-variant particles. Figure 3(b) shows a *Z*-contrast image of a CoPt nanoparticle composed of three-variant ordered domains: the *c*-axis of the central region of the particle is normal to the film plane (parallel to the electron beam, c-domain), while those of other two variants in peripheral regions of the particle are in the film plane (a, b domains). Three kinds of superlattice reflections (001a, 001b, and 110c) in the FFT pattern also explain the formation of three-variant ordered domains. Note that the nanoparticle shown in Figure 3(b) contains two (001) facets, and therefore, alternate stacking of Co(001) and Pt(001) atomic planes can be directly distinguished by *Z*-contrast in the image of a, b domains. They are both terminated by Co atomic planes as indicated by arrowheads, judging from the *Z*-contrast of Pt and Co. By contrast, Müller and Albe [24] have reported the termination of (001) planes by Pt atoms for FePt nanoparticles (TO, 2.5–8.5 nm in diameter, 50–54 at %Pt) based on Monte Carlo simulations. This discrepancy suggests that the particle shown in Figure 3(b) may not be in the thermodynamical equilibrium by annealing at 873 K for 10 h. Existence of three-variant ordered domains also indicates intermediate stage of atomic ordering [19, 25]. It is presumed that multiple nucleation of the ordered phase in a particle and a low interfacial energy between variant domains are responsible for the formation of such ordered domains. Surface segregation at {100} or {111} facets has been also discussed by Yang et al. (FePt, TO, 2.32–5.35 nm in diameter) [26] and Rossi et al. (CoPt, TO, 1.5–3 nm in diameter) [27]; however, it was difficult to detect this detailed surface atomic configuration in the present study except for the (001) planes shown in Figure 3(b).

Thus, the microscopy results indicate that postdeposition annealing at 973 K is required for realizing a highly ordered single-variant structure for the $L1_0$ CoPt nanoparticles prepared by epitaxial growth techniques using sequential deposition of Pt and Co [18]. Lowering of kinetic ordering temperature is also desired for practical applications; however, ordering rate of the Co-Pt system is slow compared to that of similar compounds such as Fe-Pt or Fe-Pd [28].

Figure 4(a) shows *Z*-contrast images for single-variant CoPt nanoparticles with size of 3–5 nm in diameter after annealing at 873 K for 1 h (sample no. 3). The beam incidence is the [001] direction (along the *c*-axis of the $L1_0$ structure). Clear (110) atomic planes of the $L1_0$ ordered structure can be seen in all the nanoparticles shown here. This is evidence of the atomic ordering in a small CoPt nanoparticle, while the degree of order is not known. It is noted that nanoparticles smaller than 3 nm showed weak superlattice reflections, indicating a low degree of order [18]. Figure 4(b) shows *Z*-contrast images of CoPt nanoparticles including structural domains. Particle sizes are comparable to those shown in Figure 4(a), while two- or three-variant domains are clearly seen in these nanoparticles. Coexistence of single-variant particles and multivariant particles in the same specimen film suggests that the interfacial energy between variant domains will be small enough to form such structural domains in a 4 nm sized particle. Furthermore, the $L1_0$ ordered domain was found in an extremely small CoPt nanoparticle, 2 nm in diameter [15]; this is also evidence of a low interfacial energy. According to our previous HRTEM observation on Fe-56 at %Pt nanoparticles, three-variant ordered domains are transformed to single domain after annealing for 24 h at 873 K [25].

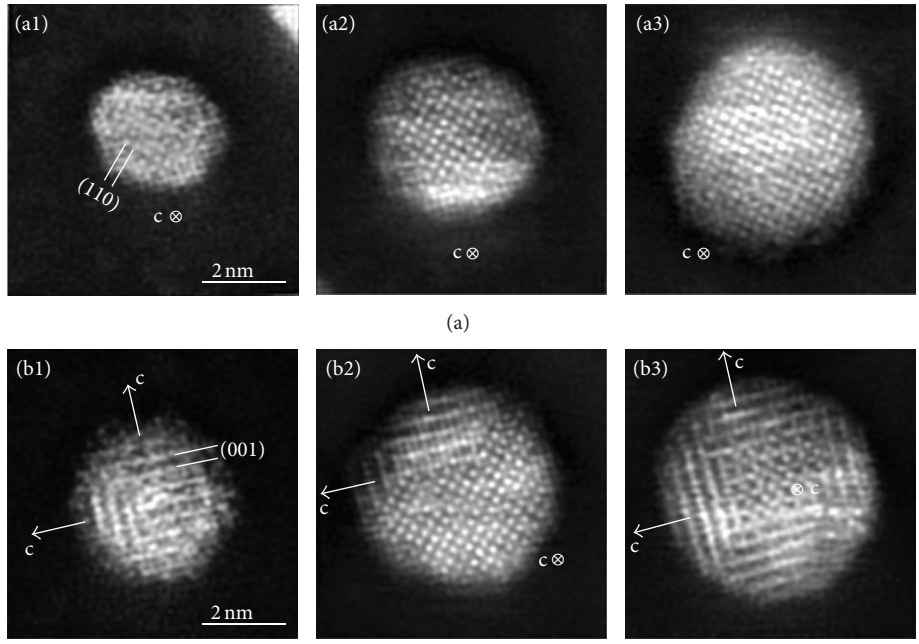

Figure 4: HAADF-STEM images of the $L1_0$-CoPt nanoparticles with sizes of 3–5 nm in diameter (sample no. 3). Annealing was performed at 873 K for 1 h. (a) Single-variant nanoparticles, (b) multivariant nanoparticles.

4. Conclusion

We have studied atomic structures of $L1_0$ CoPt nanoparticles using *Z*-contrast imaging by HAADF-STEM. Highly ordered particles are formed by high-temperature annealing at 973 K. Most of the particles are single crystal with *c*-axis oriented normal to the film plane. Image simulation revealed that HAADF-STEM image intensity is sensitive to thickness variation in addition to atomic number. On the other hand, for a specimen annealed at 873 K, nanoparticles composed of multivariant ordered domains are observed in addition to single-variant particles. It was found that (001) facets of particles with structural domains are terminated by Co atomic planes rather than by Pt, suggesting an intermediate stage of atomic ordering. Coexistence of single-variant particles and multivariant particles in the same specimen film suggests that the interfacial energy between the ordered domains will be small enough to form such structural domains in a particle as small as 4 nm in diameter. This study thus demonstrates that postdeposition annealing at 973 K is required for realizing highly ordered single-variant structure for the $L1_0$ CoPt nanoparticles prepared by epitaxial growth techniques using sequential deposition of Pt and Co.

Conflict of Interests

The authors declare no possible conflict of interests.

Acknowledgments

This study was partially supported by the Challenging Exploratory Research (Grant no. 23651094) from the Ministry of Education, Culture, Sports, Science, and Technology, Japan. The authors wish to thank Mr. E. Aoyagi and Mr. Y. Hayasaka for their help in using TEM.

References

[1] D. Weller and M. F. Doerner, "Extremely high-density longitudinal magnetic recording media," *Annual Review of Materials Science*, vol. 30, pp. 611–644, 2000.

[2] Y. Tanaka, "Fundamental features of perpendicular magnetic recording and design considerations for future portable HDD integration," *IEEE Transactions on Magnetics*, vol. 41, no. 10, pp. 2834–2838, 2005.

[3] M. A. Seigler, W. A. Challener, E. Gage et al., "Integrated heat assisted magnetic recording head: design and recording demonstration," *IEEE Transactions on Magnetics*, vol. 44, no. 1, pp. 119–124, 2008.

[4] R. Wood, M. Williams, A. Kavcic, and J. Miles, "The feasibility of magnetic recording at 10 terabits per square inch on conventional media," *IEEE Transactions on Magnetics*, vol. 45, no. 2, pp. 917–923, 2009.

[5] S. H. Liou, Y. Liu, S. S. Malhotra, M. Yu, and D. J. Sellmyer, "Magnetic properties of nanometer-size CoPt particles," *Journal of Applied Physics*, vol. 79, no. 8, pp. 5060–5062, 1996.

[6] C. Chen, O. Kitakami, S. Okanioto, Y. Shimada, K. Shibata, and M. Tanaka, "Large coercivity and granular structure of $CoPt/SiO_2$ films," *IEEE Transactions on Magnetics*, vol. 35, no. 5, pp. 3466–3468, 1999.

[7] A. Sakuma, "First principle calculation of the magnetocrystalline anisotropy energy of FePt and CoPt ordered alloys," *Journal of the Physical Society of Japan*, vol. 63, no. 8, pp. 3053–3058, 1994.

[8] H. Shima, K. Oikawa, A. Fujita et al., "Magnetocrystalline anisotropy energy in $L1_0$-type CoPt single crystals," *Journal of Magnetism and Magnetic Materials*, vol. 290-291, no. 1, pp. 566–569, 2005.

[9] T. Shima, T. Moriguchi, S. Mitani, and K. Takanashi, "Low-temperature fabrication of $L1_0$ ordered FePt alloy by alternate monatomic layer deposition," *Applied Physics Letters*, vol. 80, no. 2, pp. 288–290, 2002.

[10] S. Okamoto, N. Kikuchi, O. Kitakami, T. Miyazaki, Y. Shimada, and K. Fukamichi, "Chemical-order-dependent magnetic anisotropy and exchange stiffness constant of FePt (001) epitaxial films," *Physical Review B*, vol. 66, no. 2, Article ID 024413, pp. 1–9, 2002.

[11] K. Sato, T. J. Konno, and Y. Hirotsu, "Electron microscopy studies on magnetic $L1_0$-type FePd nanoparticles," *Advances in Imaging and Electron Physics*, vol. 170, pp. 165–225, 2012.

[12] K. Sato, J. G. Wen, and J. M. Zuo, "Intermetallic ordering and structure in Fe-Pd alloy nanoparticles," *Journal of Applied Physics*, vol. 105, no. 9, Article ID 093509, pp. 1–7, 2009.

[13] K. Sato, K. Yanajima, and T. J. Konno, "Structure and compositional evolution in epitaxial Co/Pt core-shell nanoparticles on annealing," *Thin Solid Films*, vol. 520, no. 9, pp. 3544–3552, 2012.

[14] M. Delalande, M. J.-F. Guinel, L. F. Allard et al., "$L1_0$ ordering of ultrasmall FePt nanoparticles revealed by TEM in situ annealing," *Journal of Physical Chemistry C*, vol. 116, no. 12, pp. 6866–6872, 2012.

[15] F. Tournus, K. Sato, T. Epicier, T. J. Konno, and V. Dupuis, "Multi-$L1_0$ domain CoPt and FePt nanoparticles revealed by electron microscopy," *Physical Review Letters*, vol. 110, no. 5, Article ID 055501, pp. 1–5, 2013.

[16] D. Wang, H. L. Xin, R. Hovden et al., "Structurally ordered intermetallic platinum-cobalt core-shell nanoparticles with enhanced activity and stability as oxygen reduction electrocatalysts," *Nature Materials*, vol. 12, no. 1, pp. 81–87, 2013.

[17] S. J. Pennycook and P. D. Nellist, Eds., *Scanning Transmission Electron Microscopy, Imaging and Analysis*, Springer, New York, NY, USA, 2011.

[18] K. Sato, K. Yanajima, and T. J. Konno, "Effect of cooling rate on size-dependent atomic ordering of CoPt nanoparticles," *Philosophical Magazine Letters*, vol. 92, no. 8, pp. 408–416, 2012.

[19] B. Bian, K. Sato, Y. Hirotsu, and A. Makino, "Ordering of island-like FePt crystallites with orientations," *Applied Physics Letters*, vol. 75, no. 23, pp. 3686–3688, 1999.

[20] D. Alloyeau, C. Ricolleau, C. Mottet et al., "Size and shape effects on the order-disorder phase transition in CoPt nanoparticles," *Nature Materials*, vol. 8, no. 12, pp. 940–946, 2009.

[21] http://elim.physik.uni-ulm.de/?page_id=834.

[22] T. B. Massalski, H. Okamoto, P. R. Subramanian, and L. Kacprzak, Eds., *Binary Alloy Phase Diagrams*, ASM International, Materials Park, Ohio, USA, 2nd edition, 1990.

[23] K. Sato, Y. Hirotsu, H. Mori, Z. Wang, and T. Hirayama, "Long-range order parameter of single $L1_0$-FePd nanoparticle determined by nanobeam electron diffraction: particle size dependence of the order parameter," *Journal of Applied Physics*, vol. 98, no. 2, Article ID 024308, pp. 1–8, 2005.

[24] M. Müller and K. Albe, "Lattice Monte Carlo simulations of FePt nanoparticles: influence of size, composition, and surface segregation on order-disorder phenomena," *Physical Review B*, vol. 72, no. 9, Article ID 094203, pp. 1–10, 2005.

[25] K. Sato, B. Bian, T. Hanada, and Y. Hirotsu, "Oriented $L1_0$-FePt nanoparticles and their magnetic properties," *Scripta Materialia*, vol. 44, no. 8-9, pp. 1389–1393, 2001.

[26] B. Yang, M. Asta, O. N. Mryasov, T. J. Klemmer, and R. W. Chantrell, "The nature of A1-$L1_0$ ordering transitions in alloy nanoparticles: a Monte Carlo study," *Acta Materialia*, vol. 54, no. 16, pp. 4201–4211, 2006.

[27] G. Rossi, R. Ferrando, and C. Mottet, "Structure and chemical ordering in CoPt nanoalloys," *Faraday Discussions*, vol. 138, pp. 193–210, 2008.

[28] Y. Hirotsu and K. Sato, "Growth and atomic ordering of hard magnetic $L1_0$-FePt, FePd and CoPt alloy nanoparticles studied by transmission electron microscopy: alloy system and particle size dependence," *Journal of Ceramic Processing Research*, vol. 6, no. 3, pp. 236–244, 2005.